J. Astrophys. Astr. (2000) **21**, 61–76

A New Scheme of Radiation Transfer in HII Regions including Transient Heating of Grains

S. K. Ghosh & R. P. Verma, *Tata Institute of Fundamental Research, Homi Bhabha Road, Mumbai 400005, India.*

Received 2000 April 15; accepted 2000 May 10

Abstract. A new scheme of radiation transfer for understanding the infrared spectra of HII regions, has been developed. This scheme considers non-equilibrium processes (e.g. transient heating of the very small grains, VSG; and the polycyclic aromatic hydrocarbon, PAH) also, in addition to the equilibrium thermal emission from normal dust grains (BG). The spherically symmetric interstellar dust cloud is segmented into a large number of "onion skin" shells in order to implement the non-equilibrium processes. The scheme attempts to fit the observed SED originating from the dust component, by exploring the following parameters: (i) geometrical details of the dust cloud, (ii) PAH size and abundance, (iii) composition of normal grains (BG), (iv) radial distribution of all dust (BG, VSG & PAH).

The scheme has been applied to a set of five compact H II regions (IRAS 18116 – 1646, 18162 – 2048, 19442 + 2427, 22308 + 5812, and 18434 – 0242) whose spectra are available with adequate spectral resolution. The best fit models and inferences about the parameters for these sources are presented.

Key words. HII regions—radiative transfer—PAH—VSG.

1. Introduction

Till recently, the mid to far infrared spectral energy distribution (SED) of Galactic star forming regions in general was available only in the four IRAS bands (12, 25, 60 and 100 μm). In some relatively rare cases, spectroscopy in the 10 μm band through the atmospheric window, was also available. However, the situation has changed drastically recently, due to the advent of the Infrared Space Observatory (ISO). The ISOPHOT photometer along with ISO-SWS and ISO-LWS spectrometers together has revolutionized the availability of information about SED of the astrophysical sources in general.

In the literature, several radiation transfer schemes have been used for interstellar dust clouds with embedded YSOs in spherical (e.g. Scoville & Kwan 1976; Leung 1976; Churchwell, Wolfire, & Wood 1990) as well as cylindrical (Ghosh & Tandon 1985, Dent 1988, Karnik & Ghosh 1999) geometries. All of these considered the dust grains to be in thermal equilibrium. The role of non-equilibrium processes (resulting in transient heating/excitation of grains, particularly in the vicinity of a source of UV radiation) has become evident from significant near and mid infrared continuum

emission detected in Galactic star forming regions (Sellgren 1984; Puget, Leger & Boulanger 1985, Boulanger, Baud & van Albada 1985) as well as spectral features (Leger & Puget 1984; Allamandola *et al.* 1985; Puget & Leger 1989). The importance of these processes has also been demonstrated in extragalactic nuclei/star forming regions (Moorwood *et al.* 1996; Metcalfe *et al.* 1996, Ghosh, Drapatz, & Peppel 1986). A comparison of the observed mid-IR spectral features with laboratory data, has led to the identification of a new constituent of the interstellar medium-polycyclic aromatic hydrocarbons (PAH). The enhanced continuum emission in the near and mid IR has been mainly attributed to the very small grains (VSG) of radii 10–100 Å. Hence, it is obviously important to include the non-equilibrium processes in attempting to model the observed SED of star forming regions in general. Basically, grains of very small size or a large organic molecule, with effective heat capacity comparable to the energy of a single UV photon get excited (for a short time) to an energy state well above its thermal equilibrium state corresponding to the local radiation field. The photons emitted during the de-excitation process contribute to the near/mid IR part of the SED, which shows continuum excess and emission features which are unexplained by radiative transfer models considering the emission from large grains in thermal equilibrium alone. Recently, Siebenmorgen & Krugel (1992) have attempted to quantify the properties of the dust components relevant for non-equilibrium processes (VSG & PAH), from the infrared data of sources in different astronomical environments in our Galaxy. The role of VSG on the infrared emission from externally heated dust clouds has been studied by Lis & Leung (1991). Krugel & Siebenmorgen (1994) have presented a method to model the transfer of radiation in dusty galactic nuclei, which includes the presence of VSG and PAH.

Here we present a scheme of radiative transfer developed by us which is applicable in spherical geometry. This includes, in addition to the dust grains in thermal equilibrium (of normal size, hereafter big grains or BG), the transient heating of very small grains (VSG) as well as the PAH molecules. An attempt has been made to model five compact HII regions: IRAS 18116 – 1646, 18162 – 2048, 19442 + 2427, 22308 + 5812 and 18434 – 0242 using the above scheme.

In section 2, the radiative transfer modelling scheme is briefly described. The results of modelling the five compact HII regions are presented in section 3. The last section (4) consists of discussion.

2. The modelling scheme

2.1 *Dust components and their properties*

The normal grains (BG) consist of two components: astronomical silicate and graphite. Their size distribution is taken as per Mathis, Rumpl & Nordsieck (1977) to be a power law, $n(a) \propto a^{\gamma}$, with —3.5 as the exponent. The lower and upper limits of the grain radii are taken to be 0.01 μm and 0.25 μm respectively as recommended by Mathis *et al.* (1983), for both astronomical silicate as well as graphite grains. The scattering and absorption coefficients, and anisotropic scattering factors have been taken from Draine & Lee (1984) and Laor & Draine (1993).

The VSG component is taken to be graphite grains of a single size : either 10 Å or 50 Å in radius. Their optical properties have also been taken from Draine & Lee

(1984). Abundance of VSG is connected to that of the normal grains through a scaling factor Y_{VSG}, which gives the fraction of dust mass in VSG form to the normal BG form. The value of Y_{VSG}, was taken from Desert *et al.* (1990), which is needed to account for the 2200 Å bump in the average interstellar medium in the Galaxy, and it has been held fixed for all models considered here.

The PAH component is assumed to be either a single molecule with about 15–30 atoms, or a large complex consisting of 10–20 of these molecules as used by Siebenmorgen (1993). Their optical properties, feature centres, feature shape and widths have been taken from Leger & d'Hendecourt (1987). The abundance of PAH component is also connected through a scaling factor Y_{PAH} to the normal grains (BG). There are two additional parameters explored in the modelling of the observed PAH spectral features : (i) the radius of the PAH molecule / complex, α_{PAH}; and (ii) the de-hydrogenation factor, f_{de-H}. The value of f_{de-H} lies between 0 and 1 (f_{de-H} = 0 refers to completely hydrogenated PAH). Whereas α_{PAH} has implications of heat capacity and hence the efficiency of transient heating for a given radiation field, the f_{de-H} affects the ratios of PAH features resulting from the C–H versus C=C stretch modes.

2.2 *Geometry*

The star forming region is considered as a spherical dust cloud immersed in an isotropic interstellar radiation field, with an embedded source of energy (e.g. a ZAMS star) at its centre. A central cavity in this cloud represents sublimation/destruction of grains in the intense radiation field of the central source. A schematic of the dust cloud is presented in Fig. 1. This spherically symmetric dust cloud, is divided into a large number of concentric contiguous spherical shells (say $Sh_1, Sh_2, \ldots, Sh_N$) like "onion skins". Each shell, Sh_i, is identified by its inner and outer radii (R_i^{min} and R_i^{max}; see Fig. 1). These shells can be of different selectable thicknesses, depending on the optical depth at the shortest relevant wavelength. In order to incorporate the presence of both – normal grains (BG, responsible for emission at thermal equili-

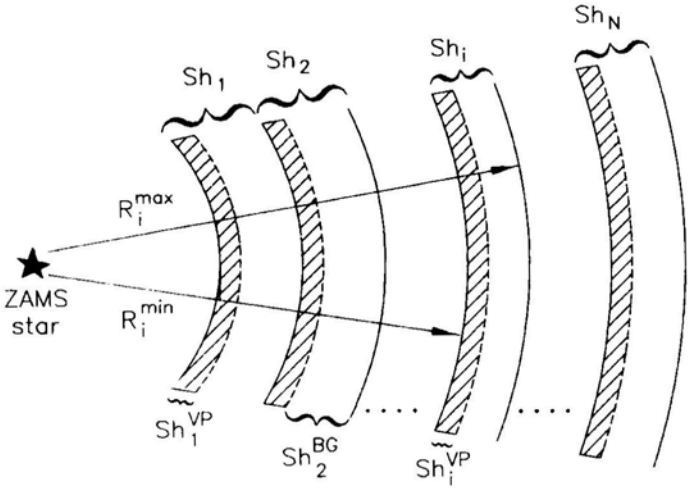

Figure 1. Schematic diagram of the shell structure of the cloud.

brium), as well as the grains responsible for non-equilibrium emission (VSG and PAH), each shell is subdivided into a pair of sub-shells, Sh_i^{BG} and Sh_i^{VP} corresponding to these two components respectively. Whereas the former consists of only BG, the latter consists of only the VSG and PAH.

The full detailed radiative transfer calculations assuming the normal grains to be in thermal equilibrium, are performed in each of the sub-shells Sh_i^{BG}, for i =1, 2, ... , N. The subshells Sh_i^{VP}, go through a statistical mechanical treatment describing the non-equilibrium emission processes for the VSGs and the PAHs. For simplicity of computations, the sub-shells Sh_i^{VP} are considered to be very thin compared to the total thickness of the shell Sh_i, and this sub-shell is assumed to be placed at the inner edge of the shell Sh_i (see Fig. 1). The final results are expected to be insensitive to the above simplification since individual shells are optically thin.

Radiative transport at each of the two sub-shells is carried out as a two point boundary value problem, the two boundary conditions being the incident radiation fields at the two surfaces. The calculations begin with the given spectrum emitted by the embedded energy source (in general, an Initial Mass Function weighted synthetic stellar spectrum ensemble) incident at the inner boundary of the first shell Sh_1. The outer surface of the last (outermost) shell, Sh_N, has the interstellar radiation field (ISRF) incident on it from the outside. Starting from the "core" side of the first shell, the radiation is transported through the sub-shell Sh_1^{VP} first and the emergent processed spectrum is considered to be incident on the other sub-shell Sh_1^{BG}. The emergent spectrum from the latter is the processed output of the entire shell Sh_1 and is used as input boundary condition for the next shell Sh_2. In this manner, the radiation field is transported outward from shell Sh_1 to Sh_2 ... till the last shell, viz., Sh_N is reached. This entire processing from shell 1, 2, ... to N, constitutes one iteration. Several such iterations (typically 5–10) are carried out until a set of predetermined convergence criteria are satisfied. The emerging spectrum from the last shell, Sh_N, is the desired output of the full model. The number of shells used for a specific source is determined by the criterion that the shell is optically thin in the shortest relevant wavelength.

2.3 *Processing of transient heating of the VSG and the PAH*

As described above, the dust components in a shell for which the non-equilibrium emission processes are important, are segregated into a separate sub-shell (Sh_k^{VP}) consisting only of the VSG and the PAH. The interaction of the total incident radiation field from both the surfaces of this sub-shell, ($I^{\nu}_{\rm in}$), with the VSG component, is considered using a code developed by us based on the statistical mechanical treatment prescribed by Desert *et al.* (1986). The incident radiation, partly extinguished by the VSGs ($I^{\nu}_{\rm VP}=I^{\nu}_{\rm in}$)$\times e^{-T^{\nu}_{\rm VSG}}$), is considered incident on the PAH component and a similar computation is repeated. The final emerging spectrum consists of three components:

- the originally incident radiation extinguished by *both* VSG as well as PAH, ($I^{\nu}_{\rm out} = {\rm I}^{\nu}_{\rm in}\times e^{-(T^{\nu}_{\rm VSG}+T^{\nu}_{\rm VSG})}$),
- the emission from the VSG component, and
- the emission from the PAH component.

Whereas the first component is direction sensitive (the two surfaces get different contributions depending on the original spectrum incident at the other surfaces), the latter two contribute equally to the two surfaces.

The VSG and PAH components of grains have fluctuating temperature, mainly because their enthalpy (internal energy) is comparable to the energy of UV or visual photons. This means, the multiphoton absorption processes can become important (depending on the exact radiation field and the details of thermal and optical properties of these grains) as they can lead to a modified temperature distribution. An iterative method has been used here to consider these multiphoton processes for VSGs and PAHs separately. The method assumes a single grain in an isotropic radiation field, and follows the evolution of the grain temperature by solving the relevant stochastic differential equation.

A scheme of between 100 to 400 levels of internal energy (covering 0.5 eV to 200 eV) for considering discrete heating/cooling processes; and 400 energy levels (for energies 1.25×10^{-3} eV to 0.5 eV) for considering the continuum processes, has been incorporated. A total of 97 frequency grid points covering 0.0944 μm to 5000μm have been used. Several grid points are densely packed around the five PAH features at 3.3, 6.2, 7.7, 8.6 and 11.3 μm.

2.4 *Radiation transport through normal grains (BG)*

Each of the sub-shells consisting of the normal grains, (Sh_k^{BG}, k = 1, 2, ... N), separately undergoes full radiative transport calculation using the code CSDUST3 developed by Egan *et al.* (1988) (see also Leung 1975). In CSDUST3, the moment equation of radiation transport and the equation of energy balance are solved simultaneously as a two-point boundary value problem. The effects of multiple scattering, absorption and re-emission of photons on the temperature of dust grains and the internal radiation field have been considered self-consistently. In addition, multi grain components, radiation field anisotropy and linear anisotropic scattering are also incorporated.

The same frequency grid of 97 points, as used for VSG and PAH, has been used here. In order to avoid non-convergence problems due to sharp changes in optical depth at any of the frequency grids, logarithmically increasing radial grid spacings have been used at the inner shell boundary. Similarly smoothly decreasing grid spacings have been used near the outer shell boundary.

2.5 *The modelling scheme*

The scheme aims to construct a model constrained by the observed SED covering the entire infrared and the sub-mm/mm region. Based on comparisons of the model predicted SEDs with the observed SED, various model parameters are fine tuned till the best fit model is identified. The following model parameters are explored:

- the total radial optical depth (represented at a fiducial wavelength of 100 μm);
- exponent of the dust density distribution power law;
- the ratio of graphite component to the astronomical silicate component for BGs;
- size of VSGs, a_{VSG}: either 50 Å or 10 Å:

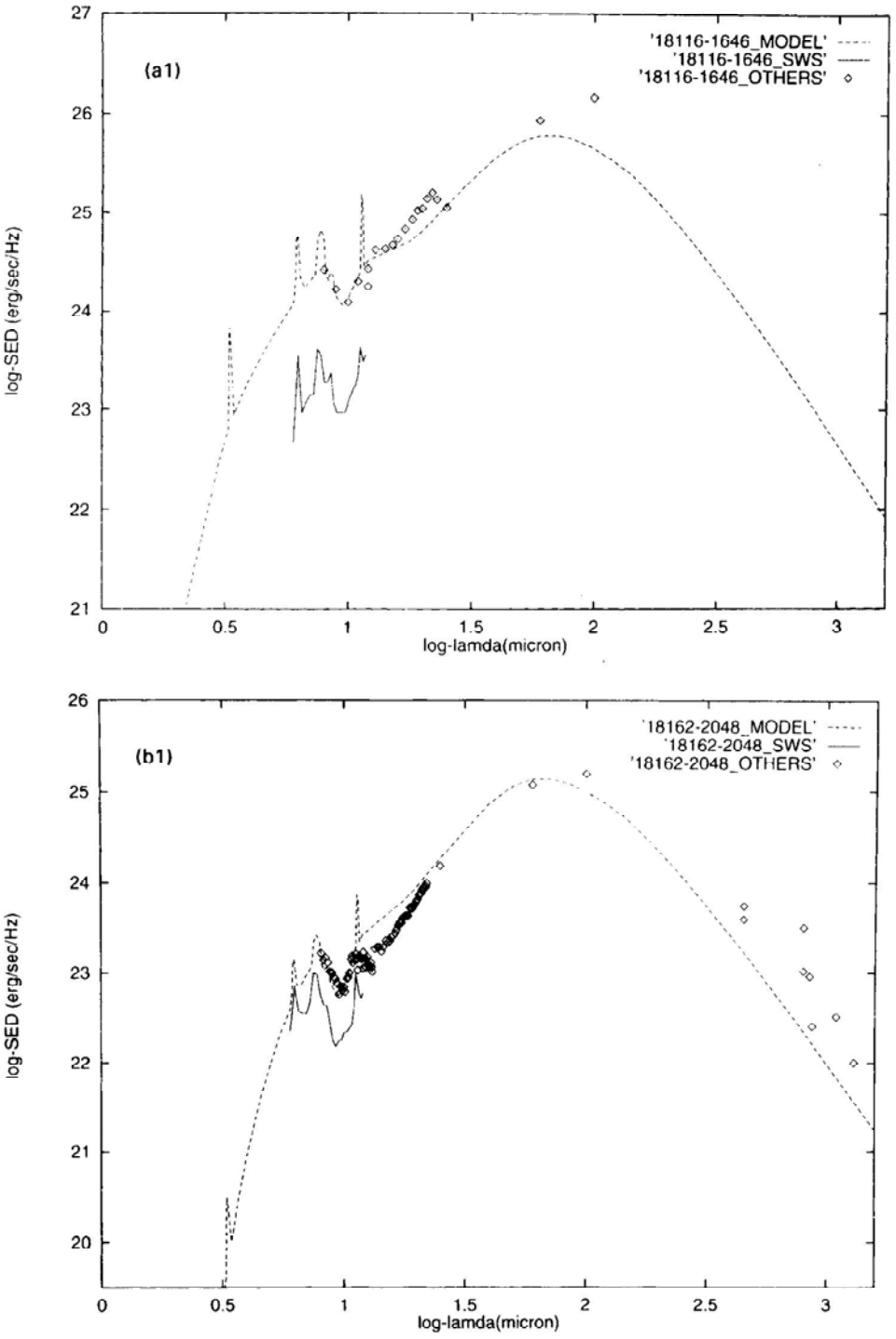

Figure 2. (*Continued*)

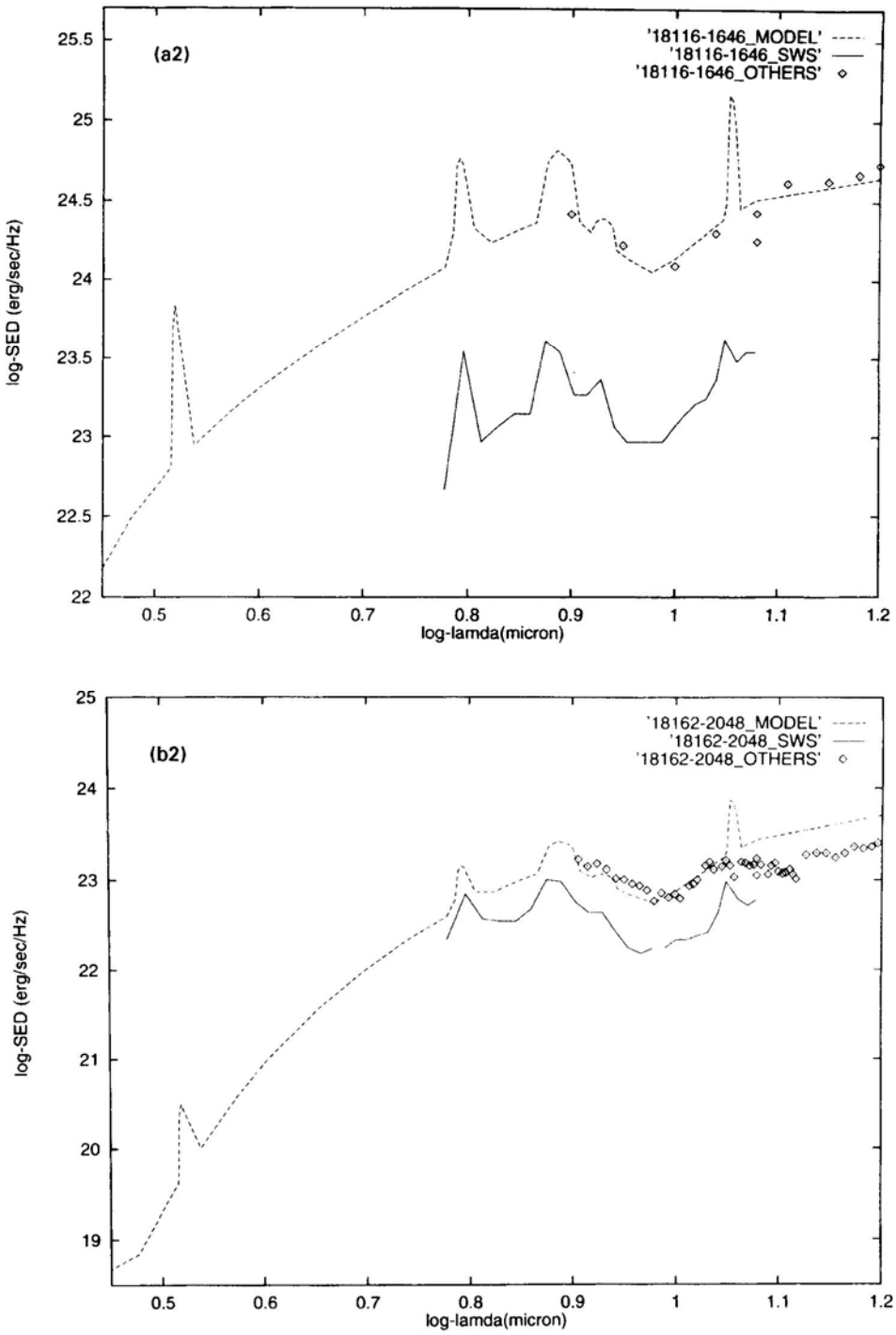

Figure 2. (*Continued*)

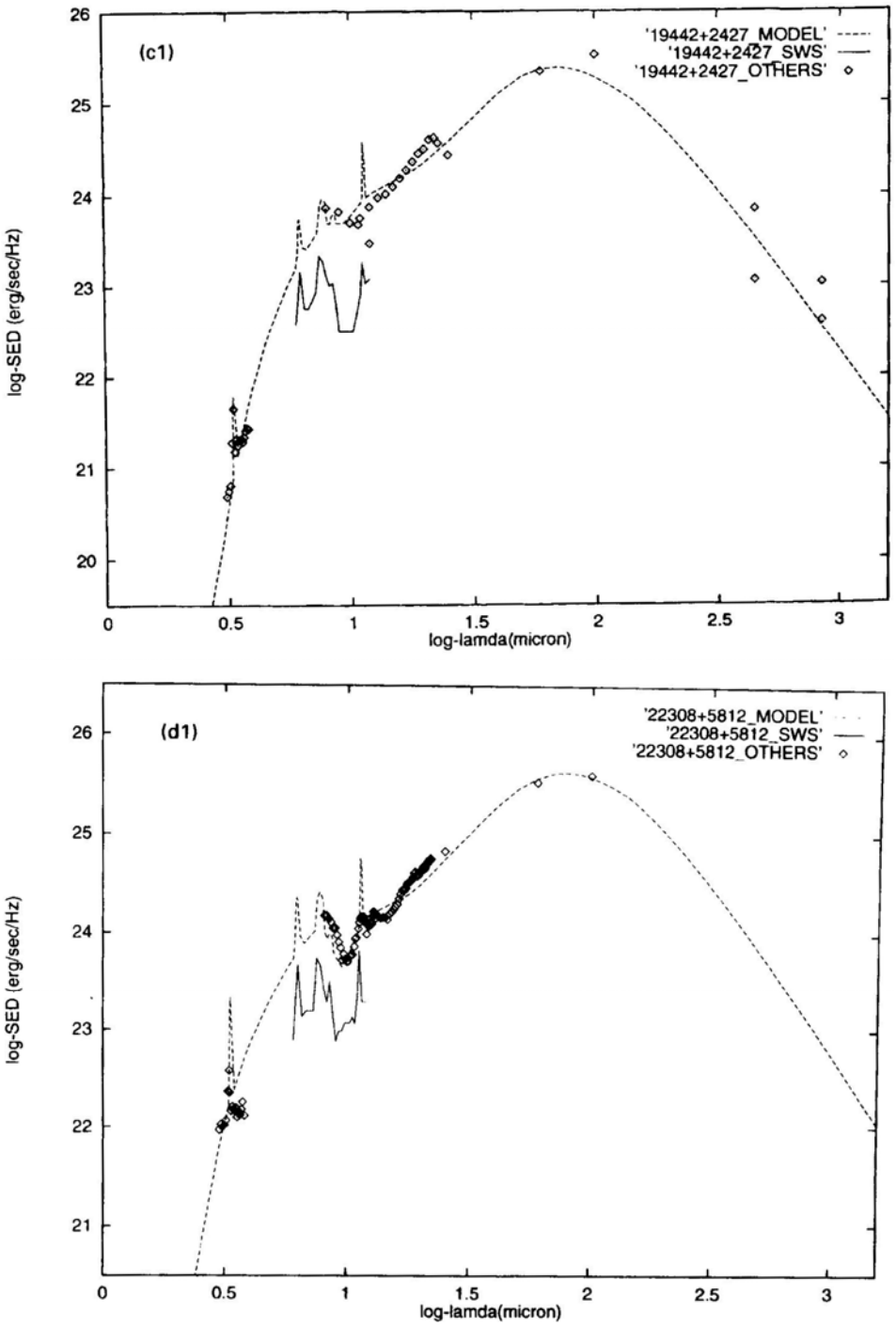

Figure 2. (*Continued*)

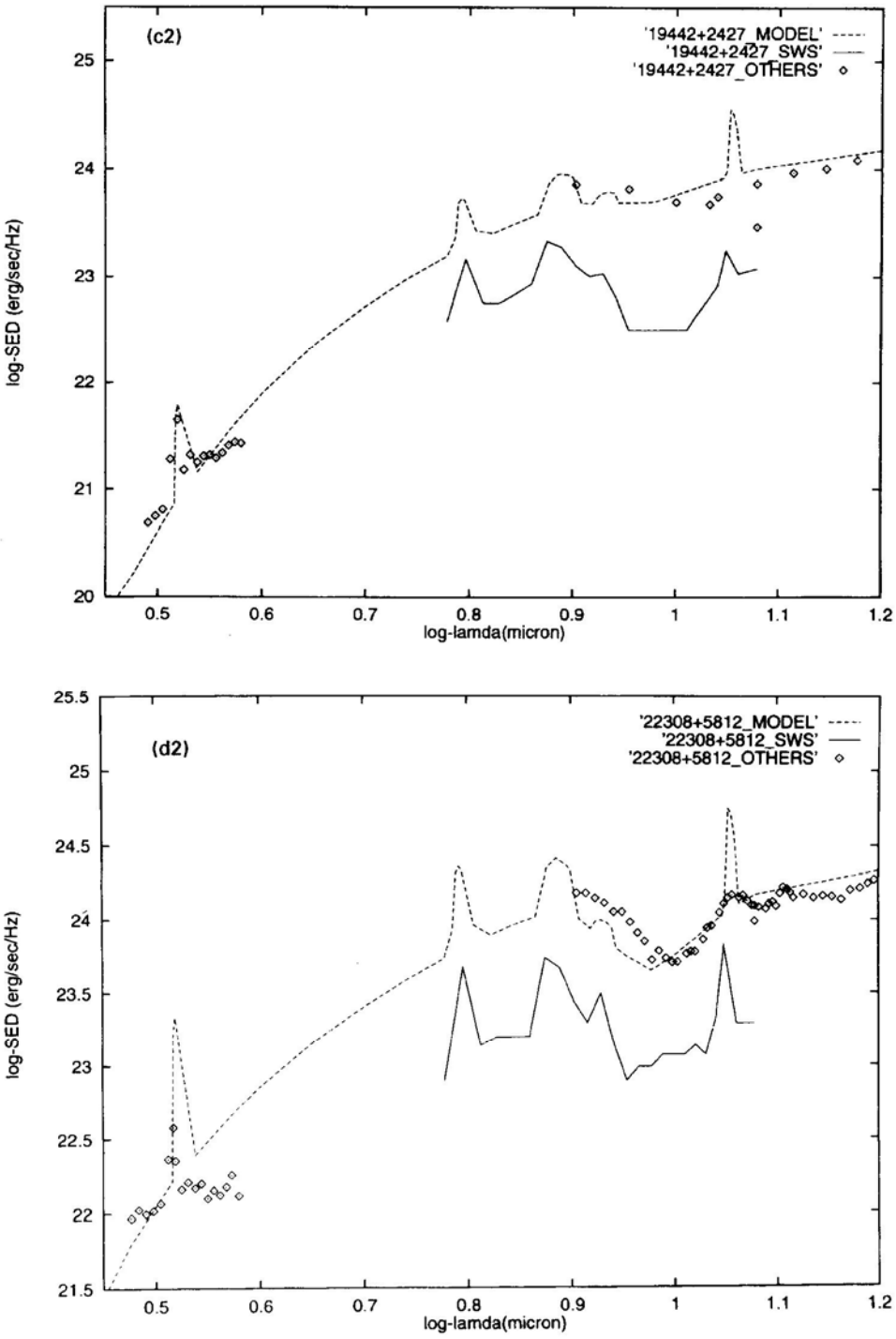

Figure 2. *(Continued)*

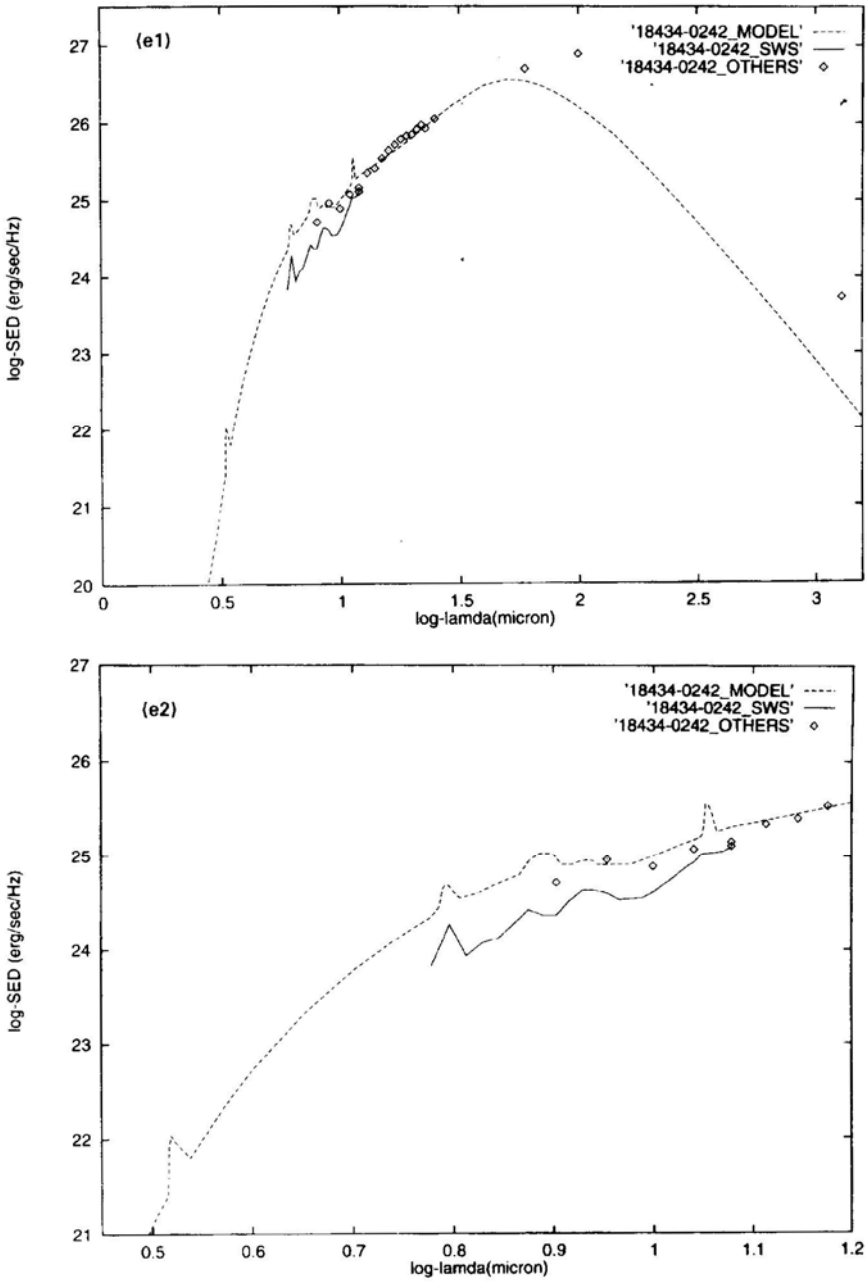

Figure 2. Spectral energy distribution of the five compact HII regions. The ordinate is the log of the flux density multiplied by the surface area of the respective cloud. Solid lines show the ISO-SWS spectra from Roelfsema *et al.* (1996); dotted lines show our best fit model spectra; diamonds show other observations. Other observations include — 3 μm observations from de Muizon *et al* (1990), IRAS LRS spectra from Olnon & Raimond (1986) or from Volk & Cohen (1989), IRAS PSC flux densities, sub-mm observations from McCutcheon *et al.* (1995), Jenness et al. (1995) or Barsony (1989), and 1.3 mm observation of Chini *et al* (1986). In order to show the PAH features clearly, mid IR region of the SEDs are shown separately.

- size of PAH molecule / cluster, a_{PAH}: 4.6 Å or 8 Å or 13.6 Å;
- relative abundance of PAH compared to BGs, Y_{PAH} (a constant or varying with the radial distance) ; and
- the de-hydrogenation factor, f_{de-H}

The inner radius (R_{in}), for each model of the spherical cloud, has been determined using the constraint that the temperature of the BG is equal to 1500 K, the sublimation temperature of the normal big grains (graphite and astronomical silicate). The radial dust density distribution law has been assumed to be a power law $n_d(r) \propto r^{-\alpha}$, and the values of α that have been explored are 0, 1 and 2.

3. Application of the modelling scheme

In order to demonstrate the usefulness of the scheme described above, an attempt has been made to apply the same to a few HII regions. The question is : in spite of rather simplistic treatment, can we get any insight into physical details of these sources?

3.1 *The sample of compact KII regions*

With the advent of Infrared Space Observatory (ISO), it has become now possible to have precise spectroscopic information in the entire infrared band encompassing near to far infrared region. The spectroscopic results for a sample of six Galactic compact HII regions, covering four of the five major PAH features have been published by Roelfsema *et al.* (1996). We have chosen five out of their six sources for our detailed study. The sixth source IRAS 21190+5140, identified with M1-78 and variously considered as HII region and planetary nebula (Puche *et al.* 1988; Acker *et al.* 1992), has not been considered here. Although the published spectral results from ISO is rather limited (6-12 μm), if the IRAS Point Source Catalog (IRAS PSC) measurements (at 12, 25, 60 and 100 μm), IRAS Low Resolution Spectra (IRAS LRS; between 8 and 22μm) and ground based spectroscopy around the 3.3 μm PAH feature, are included (whenever available), then sufficient observational constraints can be placed on the radiative transfer models. All these measurements have been compiled to construct the SEDs for the five compact HII regions, which are displayed in Fig. 2.

The total luminosity, L_{tot} has been taken from Roelfsema *et al.* (1996) for all the sources except for IRAS 18434–0242. The luminosity for IRAS 18434 — 0242 listed by them is too low compared to that estimated from the IRAS data. The latter has been used here for modelling. Assuming the embedded source to be a single ZAMS star of luminosity L_{tot}, a Planckian spectral shape with corresponding temperature taken from Thompson (1984), has been assumed and listed in Table 1. Since distance estimates are available for all these sources, angular sizes are required to fix the outer radii of the clouds. The mid infrared angular sizes are estimated by comparing the flux densities at 12 μm as measured by IRAS-LRS and the ISO-SWS and the solid angle covered by the ISO-SWS. It is assumed that the source size is smaller than the IRAS-LRS beam and has constant brightness per unit solid angle. The entire size of the cloud has been estimated from the 12μm size by using empirical relation between angular size and the wavelength for compact HII regions (Mookerjea & Ghosh 1999).

3.2 *Results of modelling*

It has been possible to get reasonable fits to the observed SEDs of all the five compact HII regions by varying parameters of our modelling scheme. The predicted spectra and the observations are compared in Fig. 2.

The following comments are valid for all the five compact HII regions studied here. It was found that the models with uniform density distribution i.e. $n(r) \propto r^0$ (as opposed to $n(r) \propto r^{-1}$ or r^{-2}) gave much better fits to the SEDs. The VSGs with a_{VSG} = 50 Å and the PAHs with intermediate size (i.e.a_{PAH} = 8 Å) give better fits to the respective spectra. The de-hydrogenation factor, f_{de-H}, needs to be zero (corresponding to $N_H = \sqrt{6 \times N_C}$) in order to fit the relative strengths of the PAH features for all the five sources. This value of f_{de-H}, is typical for the types of PAH which have been strongly proposed in the literature, viz., Coronene & Ovalene (Leger & Puget 1984). In addition, this f_{de-H}, is consistent with the value of a_{PAH} (8 Å) inferred from our modelling, since such PAHs are expected to be completely hydrogenated in the emission zones (Allamandola *et al* 1989). Table 2 lists those best fit parameters related to the various dust components, which are valid for the entire sample of compact HII regions.

It has been found that, whereas the BG and VSG components should exist throughout the cloud, it is absolutely necessary that the PAH component must be confined to a thin inner region ($R_{out}^{PAH} \ll R_{out}$), in order to reproduce the PAH features. The size of this region is quantified by a parameter η_{PAH}, which is defined as: $\eta_{PAH} = ((R_{out}^{PAH} - R_{in})/(R_{out} - R_{in}))$. This parameter had to be varied for each source, till a good fit to the spectrum was obtained. In addition, the abundance of PAH relative to BGs, $Y_{PAH,}$ needed to be increased by a factor 10 relative to the normal value

Table1. Input parameters of the compact HII regions.

IRAS Source	L ($L_\odot$)	T_* (K)	D_{sun} (kpc)	θ_{dia} ($''$)	R_{out} (pc)
18116 − 1646	1.6×10^5	40,000	4.4	105	1.12
18162 − 2048	2.8×10^4	30,900	1.9	63	0.29
19442 + 2427	5.4×10^4	35,500	2.3	93	0.52
22308 + 5812	8.8×10^4	37,500	5.7	95	1.31
18434 − 0242	1.0×10^6	48,000	7.4	38	0.69

Table. 2. Dust parameters valid for the entire sample of compact HII regions.

Dust component	Parameter (unit)	Value
BG	a_{min} (μm)	0.01
	a_{max} (μm)	0.25
	γ	−3.5
VSG	a_{VSG} (Å)	50.0
	Y_{VSG}	4.70×10^{-4}
PAH	a_{PAH} (Å)	8.0
	Y_{PAH}	4.30×10^{-3}
	f_{de-H}	0.0

Table 3. Best fit parameters of the compact HII regions as determined by modelling.

IRAS source name	R_{in} (pc)	R_{out} (pc)	n_H (cm^{-3})	M_{Tot} ($M_\odot$)	τ_{100}^{tot}	Graphite : Silicate (% : %)	η_{PAH}
18116 − 1646	1.4×10^{-3}	1.12	1.32×10^{4}	1.9×10^{3}	0.056	75 : 25	2.1×10^{-2}
18162 − 2048	5.3×10^{-4}	0.29	1.32×10^{5}	3.3×10^{2}	0.14	88 : 12	2.7×10^{-2}
19442 + 2427	7.5×10^{-4}	0.52	5.30×10^{4}	7.7×10^{2}	0.10	95 : 5	1.5×10^{-2}
22308 + 5812	1.5×10^{-3}	1.31	1.38×10^{4}	3.2×10^{3}	0.068	77 : 23	1.3×10^{-2}
18434 − 0242	2.2×10^{-3}	0.69	5.30×10^{4}	1.8×10^{3}	0.14	95 : 5	5.5×10^{-2}

obtained by Desert *et al.* (1990). However this does not lead to any conflict with the available carbon, since $\eta_{\rm PAH} \ll 1$. The values of the best fit parameters specific to each source, are presented in Table 3.

4. Discussion

The following inferences can be drawn about the sources modelled here, provided the basic assumptions (e.g. spherical symmetry; sources of energy located only at the centre of the cloud; etc.) are not at great variance from the reality.

The most favoured radial dust density distribution law, *for all five sources,* turns out to be of uniform density. This can perhaps be understood in terms of the far infrared constraints (IRAS-PSC 60 and 100 μm data). If the dust density is falling with radial distance, then in order to fit the FIR part of the SED, so high a dust density is required at the vicinity of the embedded ZAMS star, that the mid infrared emission becomes invisible. This problem can perhaps be avoided in a non-spherically symmetric geometry. We have explored the effects of relaxing the assumption that $R_{\rm in} = R_0$, where R_0 is the radial distance at which (BG) grain temperature becomes equal to the sublimation temperature (1500 K). The most important effect of making $R_{\rm in} > R_0$ is to drastically modify the near and mid infrared continuum level of the predicted spectrum. In addition, the role of non-equilibrium processes vis-a-vis thermal equilibrium emission of the PAH features, as well as the continuum due to VSG, changes significantly.

A quick perusal of Figure 2 and Tables 2 and 3 brings out the following facts:

- All the compact HII regions considered here, are deeply embedded stars; total optical depth at 100 μm in the range of 0.056-0.14. This is necessary to explain the far IR spectra observed by IRAS.
- PAH is confined only to a thin central shell; the thickness of this shell being just a few per cent (1.3 — 5.5%) of the total thickness of the dust cloud. As these sources are optically thick at mid IR, if the PAH is distributed throughout the cloud, its emission which occurs in the inner hot region where high energy photons responsible for non-equilibrium processes are present, will be absorbed by the outer cooler shells, and PAH features will not be detectable.
- The BGs are dominated by graphites, with silicates contributing less than 25%. The latter has been tied down rather precisely by the 10 μm silicate feature.
- ISO-SWS fluxes are generally much smaller than IRAS fluxes at similar wavelengths, indicating that SWS is not sampling full emission at mid IR and the source sizes at these wavelengths are much larger than the SWS beam size (14″ x 20″). With this in mind, we have not tried to fit the absolute fluxes of the SWS but only used its shape as indicative of the importance of PAH molecules.

The following comments can be made about the individual sources:

IRAS 18116-1646: It has relatively lower optical depth. The fit to the IR data is quite reasonable, except at 100 μm where IRAS flux is higher; no sub-mm observation exists for this source.

IRAS 18162-2048: This source (GGD27) was originally thought to be a HH object. However now it has been established as a star forming region with

reflection nebulosity as well as outflow (see for example Stecklum *et al.* 1997). The region has several near IR and mid IR sources; the source of energy being close to IRS2. The size of this source at sub-mm wavelengths is ~ 1' (McCutcheon *et al.* 1995), consistent with the size for the best fit model. The mass of the envelope estimated by our model is not far from the estimate of Yamashita *et al.* (1987), viz., $200M_{\odot}$. They have proposed a disk geometry for this source. This source has very high optical depth. The fit to the IR data is quite reasonable but at the sub-mm wavelengths the calculated flux densities are lower than the observed ones.

IRAS 19442+2427: This source lies in the HII region S87. The size of this source at sub-mm wavelengths is ~1′ (Jenness *et al.* 1995), consistent with the size for the best fit model. This source has medium optical depth. The fit to all the observations from 3 μm to 850 μm is quite reasonable.

IRAS 22308+5812: It has relatively lower optical depth. The fit to the IR data is quite reasonable; no sub-mm observation exists for this source.

IRAS 18434–0242 : This source is the most luminous source with high optical depth. There are no IR observations for this source other than those from IRAS and ISO. IRAS PSC 100 μm as well as 1.3 mm observations are higher than calculated.

From the above, we conclude that our new scheme of radiative transfer which includes non-equilibrium processes (transient heating of the grains /PAH/ VSG) in addition to the emission in thermal equilibrium, can give important physical insight into Galactic star forming regions. If the simplifying geometrical assumptions of our scheme are valid, then several important inferences can be made about the five compact HII regions considered for modelling here.

Acknowledgements

It is a pleasure to thank Bhaswati Mookerjea for her help in preparing some input parameters.

References

Acker, A., Marcout, J., Ochsenbein, F., Stenholrn, B., Tylenda, R. 1992, *Strasbourg-ESO Catalogue of Galactic Planetary Nebulae* (Munchen, ESO).
Allamandola, L. J., Tielens, A. G. G. M., Barker, J. R. 1985, *Astrophys. J. (Lett),* **290**, L25.
Allamandola, L. J., Tielens, A. G. G. M., Barker, J. R. 1989, *Astrophys. J. (Suppl.),* **71,** 733.
Barsony, M. 1989, *Astrophys. J.,* **345,** 268.
Boulanger, F., Baud, B., van Albada, G. D. 1985, *Astr. Astrophys.,* **144,** L9.
Chini, R., Krugel, E., Kreysa, E. 1.986, *Astr: Astrophys.,* **167,** 315.
Churchwell, E., Wolfire, M. G., Wood, D. O. S. 1990, *Astrophys. J.,* **354,** 247.
de Muizon, M. J., d'Hendecourt, L. B., Geballe, T. R. 1990, *Astr. Astrophys.,* **227,** 526.
Dent, W. R. F. 1988, *Astrophys. J.,* **325,** 252.
Desert, F. X., Boulanger, F., Puget, J. L. 1990, *Astr. Astrophys.,* **237,** 215.
Desert, F. X., Boulanger, F., Shore, S. N. 1986, *Asti: Astrophys.,* **160,** 295.
Draine, B. T., Lee, H. M. 1984, *Astrophys. J.,* **285,** 89.
Egan, M. P., Leung, C. M., Spagna, G. F. 1988, *Computer Physics Communications,* **48,** 271.

Ghosh, S. K., Drapatz, S., Peppel, U. C. 1986, *Astr, Astrophys.,* **167**, 341.
Ghosh, S. K., Tandon, S. N. 1985, *Mon. Not. R. Astr Soc.,* **215**, 315.
Jenness, T., Scott, P. F., Padman, R. 1995, *Mon. Not. R. Astr. Soc.,* **276,** 1024.
Karnik, A. D., Ghosh, S. K. 1999, *J. Astrophys. Astr.,* **20,** 23.
Krugel, E., Siebenmorgen, R. 1994, *Astr. Astrophys.,* **282,** 407.
Laor, A., Draine, B.T. 1993, *Astrophys. J.,* **402,** 441.
Leger, A., d'Hendecourt, L. 1987, *PAH and Astrophysics* (eds.) A. Leger, L. d'Hendecourt & N. Boccara, p 223.
Leger, A., Puget, J. L. 1984, *Astr. Astrophys.,* **137,** L5.
Leung, C. M. 1975, *Astrophys. J.,* **199,** 340.
Leung, C. M. 1976, *Astrophys. J.,* **209,** 75.
Lis, D. C., Leung, C. M. 1991, *Icarus,* **91,** 7.
Mathis, J. S., Mezger, P. G., Panagia, N. 1983, *Astr. Astrophys.,* **128,** 212.
Mathis, J. S., Rumpl, W., Nordsieck, K. H. 1977, *Astrophys. J.,* **217,** 425.
McCutcheon, W. H., Sato, T., Purton, C. R., Matthews, H. E., Dewdney, P. E. 1995, *Astr. J.,* **110,** 1762.
Metcalfe, L., Steel, S. J., Barr, P., *et al.* 1996, *Astr. Astrophys.,* **315,** L105.
Mookerjea, B., Ghosh, S. K. 1999, *Bull. Astr Soc. India,* **27,** 567.
Moorwood, A. F. M., Lutz, D., Oliva, E., *et al.* 1996, *Astr. Astrophys.,* **315,** L109.
Olnon E M., Raimond, E. (IRAS Science Team) 1986, *Astr: Astrophys. (Suppl.),* **65,** 607.
Puche, D., Zijistra, A. A., Boettcher, C., *et al.* 1988, *Astr Astrophys.,* **206,** 89.
Puget, J. L., Leger, A. 1989, *Annu. Rev. Astron. Astrophys.,* **27,** 161.
Puget, J. L., Leger, A., Boulanger, F. 1985, *Astr. Astrophys.,* **142,** L19.
Roelfsema, P. R., Cox, P., Tielens, A. G. G. M., *et al.* 1996, *Astr. Astrophys.,* **315,** L289.
Scoville, N. Z., Kwan, J. 1976, *Astrophys. J.,* **206,** 718.
Sellgren, K. 1984, *Astrophys. J.,* **277,** 623.
Siebenmorgen, R. 1993, *Astrophys. J.,* **408,** 218.
Siebenmorgen, R., Krugel, E. 1992, *Astr. Astrophys.,* **259,** 614.
Stecklum, B., Feldt, M., Richichi, A., Calamai, G., Lagage, P.O. 1997, *Astrophys. J.,* **479,** 339.
Thompson, R. I. 1984, *Astrophys. J.,* **283,** 165.
Volk, K., Cohen, M. 1989, *Astr. J.,* **98,** 931.
Yamashita, T., Sato, S., Nagata, T., Suzuki, H., Hough, J. H., McLean, I. S., Garden, R., Gatley, I. 1987, *Astr Astrophys.,* 177, 258.